Author's Accepted Manuscript

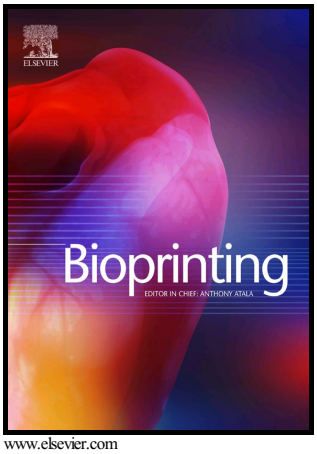

www.elsevier.com

3D Bioprinting of stimuli-responsive polymers synthesised from DE-ATRP into soft tissue replicas

Ahmed Aied, Wenhui Song, Wenxin Wang, Abdulrahman Baki, A Sigen

PII: S2405-8866(17)30021-0
DOI: https://doi.org/10.1016/j.bprint.2018.02.002
Reference: BPRINT20

To appear in: *Bioprinting*

Received date: 2 October 2017
Revised date: 29 December 2017
Accepted date: 13 February 2018

Cite this article as: Ahmed Aied, Wenhui Song, Wenxin Wang, Abdulrahman Baki and A Sigen, 3D Bioprinting of stimuli-responsive polymers synthesised from DE-ATRP into soft tissue replicas, *Bioprinting,* https://doi.org/10.1016/j.bprint.2018.02.002

3D Bioprinting of stimuli-responsive polymers synthesised from DE-ATRP into soft tissue replicas

Ahmed Aied, Wenhui Song, Ahmed Aied, Wenhui Song, Wenxin Wang, Abdulrahman Baki,A Sigen

UCL, 9th floor division of royal free hospital, Division of surgery and interventional science, United Kingdom

Abstract

Synthetic polymers possess more reproducible physical and chemical properties than their naturally occurring counterparts. They have also emerged as an important alternative for fabricating tissue substitutes because they can be molecularly tailored to have vast array of molecular weights, block structures, active functional groups, and mechanical properties. To this date however, there has been very few successful and fully functional synthetic tissue and organ substitutes and with the rapidly spreading 3D printing technology beginning to reshape the tissue engineering and regenerative field, the need for an effective, safe, and bio printable biomaterial is becoming more and more urgent. Here, we have developed a synthetic polymer from controlled living radical polymerization that can be printed into well-defined structures. The polymer showed low cytotoxicity before and after printing. Additionally, the incorporation of gelatine-methacrylate coated PLGA microparticles within the hydrogel provided cell adhesion surfaces for cell proliferation. The results point to possible application of the microparticle seeded, synthetic hydrogel as a direct printable tissue or organ substitute.

Keywords: Bioprinting, Tissue Engineering, Hydrogels, Synthetic polymer

Introduction

The complexity of biological tissues and organs is not limited to chemical and biological compositions but also in structure and configuration. Although significant achievements have been made using three-dimensional scaffolds for certain tissues [1], more complex structures such as liver, kidneys and heart are more difficult to reproduce. It is thus important that for efficient replication of tissues and organs, smart and computerised methods of fabrication are used. Three-dimensional printing offers the capability to fabricate highly complex and intricate anatomical structures that would not be possible by any other method. The process of printing 3D constructs using layer-by-layer deposition with or without automation has been around for more than three decades [2]. However, the application of this technology in the medical sector only emerged in the early 2000s with the introduction of inkjet printing of viable cells [3-5]. This quickly led to the printing of bone defects, stents and splints, and the first 3D printed blood vessels [6-8] . Today 3D printing has gained enough momentum to foster new investments in complex 3D bioprinting machines specifically designed for the detailed printing of cell laden structures. The most common methods of 3D boiprinting are inkjet and microextrusion based printing. Microextrusion printers use pneumatic[9] or mechanical (piston or screw)[10] dispensing systems to extrude continuous strands of material and/or cells. Moreover, microextrusion printing requires different material property requirement which may include thermoresponsive hydrogels, photocurable polymers, or cell pellets [11]. This allows for printing of semi-solid materials that can temporarily hold their shape and structure post printing unlike the inkjet base method. However, this can be a double edged sword since viscous and semisolid materials require more pressure to be extruded out; cell viability is compromised particularly when using small gauge needles due to shear stress

[12]. Additionally, printed materials need to be strong enough to support the weight of the upper layers. To achieve maximum structural strength post printing, stimuli responsive polymers are generally used. There are a number of naturally occurring materials that can be utilised for such propose including gelatin, collagen [5], alginate [13], and fibrin [14]. However, most of these naturally occurring materials have limited mechanical strength for most clinical applications. To overcome this, chemical modification to likes of gelatin yielded mechanically stable and printable material [15], but the biggest issue concerning biological risk and rejection remains [16]. While natural hydrogels are largely considered to be the most effective forms of chronic wound therapy, safety concerns and difficulty in scale-up continue as potential constraints natural hydrogel therapies. Thus, the design and synthesis of synthetic hydrogels with well-defined compositions, architectures, and functionalities that promote cell survival and proliferation is a challenging task in materials science.

To overcome the complications associated with naturally occurring polymers such as immunogenicity and structural integrity, we synthesised a unique copolymer with functional vinyl groups using controlled chain growth (in situ Deactivation-enhanced atom transfer radical polymerisation, DE-ATRP) [17]. This method of synthesis provides greater control over the reaction conditions and yields polymers that accurately depict the required properties such as molecular weight and polydispersity index. Moreover, we can control the branching degree without causing gelation. We opted to use hyperbranched polymers because compared to linear polymers, hyperbranched display a number of unique advantages, such as low solution and melt viscosity, and high functionality [18, 19]. By controlling the branching and preventing gelation, the vinyl functional groups (contributed by the poly (ethylene glycol) diacrylate component of the polymer) enable the copolymer the capability of easy tailoring and photo-crosslinkable property. Furthermore, the PEG based structure which is often considered to be nontoxic, nonimmunogenic and have a bio-compatible composition [20, 21] but its inert nature means it can as protein repellent, preventing interaction with extracellular

proteins and cell attachment. This drawback was circumnavigated by the impregnation of gelatine-methacrylate (gel-MA) coated PLGA microparticles (MPs) in the hydrogel to promote cell adhesion and proliferation. To synthesise a polymer that supports cell growth and is 3D printable undoubtedly offers new opportunities for the development of functional synthetic tissue equivalents.

Methods

Polymer Synthesis and characterisation

The PEGMEMA–MEO_2MA–PEGDA copolymer was synthesised by the copolymerising of PEGMEMA, MEO_2MA and PEGDA via an in situ deactivation-enhanced atom transfer radical polymerisation approach. Briefly, PEGMEMA (7.4 g, 0.015 moles), MEO_2MA (12.8 g, 0.068 moles), PEGDA (5.4 g, 0.021 moles), the initiator ethyl 2-bromoisobutyrate (155 µl, 0.001 moles), copper (II) chloride (0.032 g, 0.0002 moles), bis(2-dimethylaminoethyl)methylamine (64 µl, 0.0002 moles) were added to a two-neck flask in 25 ml solvent butanone. The mixture was stirred for complete dissolution followed by purging with argon for 30 minutes to remove dissolved oxygen. L-Ascorbic acid (0.011 g) was added to the polymerisation solution under argon conditions and the mixture was heated in an oil bath to 50°C and stirred for 6 hours. The polymerisation was stopped by opening the flask and exposing the catalyst to air. After the polymerisation, the solution was diluted with (1:1) acetone and precipitated into a large excess of diethyl ether and hexane (1:1.2) to remove solvent and monomers. The precipitated mixture of the polymer was dissolved in deionised water and purified by dialysis (spectrum dialysis membrane, molecular weight cut-off 6,000 to 8,000 CO-M_w) for 72 hours in a dark environment at 4°C against fresh deionised water, while the water was changed regularly. The pure polymer samples were obtained after freeze drying. The molecular weight and molecular weight distributions were determined for PEGMEMA–MEO2MA–PEGDA using gel permeation chromatography (Polymer Laboratories) (Amherst, MA, USA) with an (Refractive Index) detector using

dimethylformamide as an eluent. The columns (30 cm PLgel Mixed-C, two in series) were calibrated with poly (methyl methacrylate) standards. All calibrations and analysis were performed at 60°C and a flow rate of 1 ml/minute. ^{1}HNMR was carried out for PEGMEMA–MEO2MA–PEGDA on a 300 MHz Bruker NMR with Mestrenova processing software. The chemical shifts were referenced to the lock chloroform ($CDCl_3$) for PEGMEMA–MEO2MA–PEGDA (Sigma,).

Preparation of PLGA Microspheres:

Poly glycolic-co-lactic acid (PLGA 8515, 52 KDa, Evonik- USA) microspheres were prepared similar to a preparation method reported earlier by White et.al (White, Kirby et al. 2013). Briefly, 20% (w/v) PLGA solution in dichloromethane (DCM, Fischer, UK) was poured into 0.3% (w/v) polyvinyl alcohol (PVA, 86-89% hydrolysed Alfa Aesar-USA) solution and homogenised at 3000 RPM for 2 minutes using a propeller homogeniser (Silverson L5M, UK). The resultant (o/w) emulsion was left stirring overnight to allow DCM solvent evaporation. PLGA microspheres were later centrifuged (MSE Mistral 1000, UK)and washed twice with distilled water (DW), freeze-dried for 48 hours (ModulyoD, Thermo fisher scientific, USA) and stored in a vacuum packed containers at (-20 °C).

Surface Modification of PDLLGA Microspheres: Gelatine methacrylate (gel-MA) is prepared following a recently published method [22].

Low pressure oxygen plasma etching treatment was performed to introduce active oxygen species to the surface. Briefly, 500 mg of P_{DL}LGA microspheres were put in empty 25ml glass vials in a plasma machine chamber and kept rotating at 60 rpm using a special rotary holder. Chamber pressure was pumped down to 20 mbar then oxygen gas was pumped into the chamber for 2 minutes to obtain a working pressure of 50 mbar. As working pressure was maintained at 50 mbar with continuous oxygen gas supply, plasma activation was initiated at full electrode power at 100 KW for 5 minutes. Following plasma activation, chamber was purged with nitrogen gas for 2 minutes to dispose reactive oxygen ions and then air vented to

atmospheric pressure to collect the samples. Following plasma treatment, PLGA MPs were dispersed in 2 ml of gel-MA solution (10%) and kept stirring for 24 hours to allow enough time for surface modification. Treated microspheres were later washed twice with water, freeze-dried, and stored at -20 °C for later analysis (Methods 2).

3D bioprinting procedure

To make the polymer more semi-solid than viscous, 5% sacrificial porcine gelatin (sigma, UK) was added to 15% polymer solution and stored at 4°C for 20 minutes until a clear gel of polymer was formed. This mixture either contained 30% PLGA MPs or did not. Specialised pressure syringes were filled with this polymer combination and printed using the RegenHu 3D BioDiscovery printer at constant pressure, strand diameter and print-head speed. To crosslink the polymeric hydrogels we used 0.1% final concentration of Irgacure 2959 (2-Hydroxy-4'-(2-hydroxyethoxy)-2-methylpropiophenone)) for its rapid activity. UV (power: 15 W; λ: 365 nm; working distance: 35 mm; UVP Cambridge, UK) was shone for 1 min per layer during printing.

Tensile testing of hydrogels

The tensile properties the hydrogels were measured at room temperature using a Universal Texture Analyser (TA-HD Plus, Stable Microsystems, USA). The grip section of each dumbbellshaped gel was wrapped with paper towel to improve gripping. A constant deformation speed of 0.5 mm s−1 was applied during the test. The tests were stopped after the samples broke. The initial grip separation was set at 10 mm.

Mammalian cell viability

The LIVE/DEAD® Cell Viability Assay (ThermoFisher scientific) was performed to evaluate the metabolic activity of NIH/3T3 fibroblasts in the 3D cell culture system. The NIH/3T3 fibroblasts (Four million cells per milliliter were used) were encapsulated in 3D hydrogels as described above. At each time point, cells were washed with PBS at 37°C, following the addition of 2 µM calcein AM and 4 µM EthD-1 solution to the wells containing hydrogel

constructs to assess the cell viability after 0,1, 4, and 7 days. The cells in 3D construct were visualised with Leica DM IRB Inverted Fluorescence Microscope and live cells to dead cells ratio was determined using ImageJ from three images taken from different regions of the well. The data obtained from the images was used to determine cell viability and proliferation.

Statistical analysis

All data are expressed as mean ± standard deviation of triplicate samples. Comparisons between multiple groups were performed using one-way ANOVA. All analyses were performed with GraphPad Prism 5 (CA, USA). Differences between two datasets were considered significant when $P < 0.05$.

Results

The facile and versatile approach to the formation of highly branched polymer architectures through a reversible activation (or deactivation) controlled polymerization of multifunctional vinyl monomer is a significant discovery [23]. This strategy overcomes the published limitations, and most importantly, there is no restriction on the concentration of multifunctional vinyl monomer. Moreover, multifunctional vinyl monomers can even be homopolymerized to form hyperbranched polymer structures rather than cross-linked networks. The key has been to find a method for slow growth of each independent and complex hyperbranched molecule that avoids cross-linking. For the copolymerisation of Poly ($PEGMEMA_{500}$-co-MEO_2MA-co-$PEGDA_{258}$) (termed PMP), in situ DE-ATRP is used to prevent gelation and obtain yields above 50% (Table 1) which are normally not possible using conventional radical polymerisation. Moreover, a polymer with high molecular weight and branching degree is obtained (Figure 1). These properties become important in the physical behaviour of the hydrogel. For example, higher branching degree means more functional groups for further characterisation.

Table 1. Copolymerisation of poly(ethylene glycol) methyl ether methacrylate (PEGMEMA), 2-(2-methoxyethoxy)ethyl methacrylate (MEO_2MA) and poly (ethylene glycol) diacrylate (PEGDA) *via* in situ deactivation enhanced ATRP.

Monomer feed molar ratio [a] [$PEGMEMA_{500}$]:[MEO_2MA]:[$PEGDA_{258}$]	Time point (h)	Conversion [b] (%)	Mn (g/mol)	Mw (g/mol)	PDI	Vinyl content (%)[c]	Branching degree (%)[c]
15:70:15	1	31.7	7410	10863	1.47		
	2	50.5	12073	20940	1.73		
	2.5	56.8	14044	28401	2.02		
After purification			16829	35957	2.14	8.1	8.7

[c] Calculated by ^{1}H NMR.

[a] Polymerization condition: [I]: [$PEGMEMA_{500}$]:[MEO_2MA]:[$PEGDA_{258}$]:[$CuCl_2$]:[L]:[R]=1:15:70:15:0.25:0.25:0.125. Initiator: Ethyl 2-bromoisobutyrate, Legend: N, N, N′, N″, N″- Pentamethyldiethylenetriamine, Reducing agent: ascorbic acid, temperature: 50℃, Solvent: butanone.

[b] Conversion was determined by GPC.

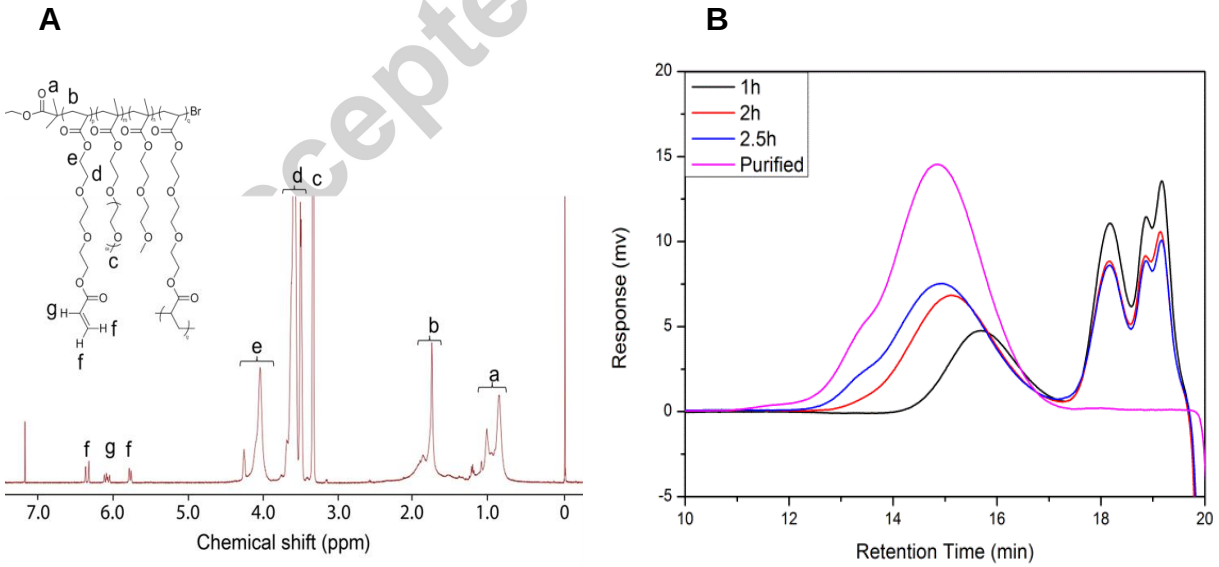

Fig 1: The polymer structure was determined using proton NMR (A) and the molecular weight and polydispersity index were measured using Gel Permeation Chromatography (GPC) (B). Proton NMR samples were taken at the end of the reaction while GPC runs were taken at half-hour intervals to monitor the reaction progress.

We measured the tensile properties of the polymer with different concentrations and compared it to gel-MA. The tensile properties of these materials were assessed using moulded dumbbell-shaped samples, and are shown in Figure 2. The modulus and strain of the gels increased when increasing the concentration. The gels showed an increase in all three mechanical properties (modulus, ultimate tensile strength, and failure strain) compared to gel-MA gels, with a maximum 80% increase in elastic modulus. While higher concentrations can further increase the modulus and strength of gels, they can also reduce the transportation of nutrients [24-26] and cell viability [27, 28]. The biocompatibility of bio-inert hydrogels (including the one reported here) has been previously reported in the clinical setting [29].

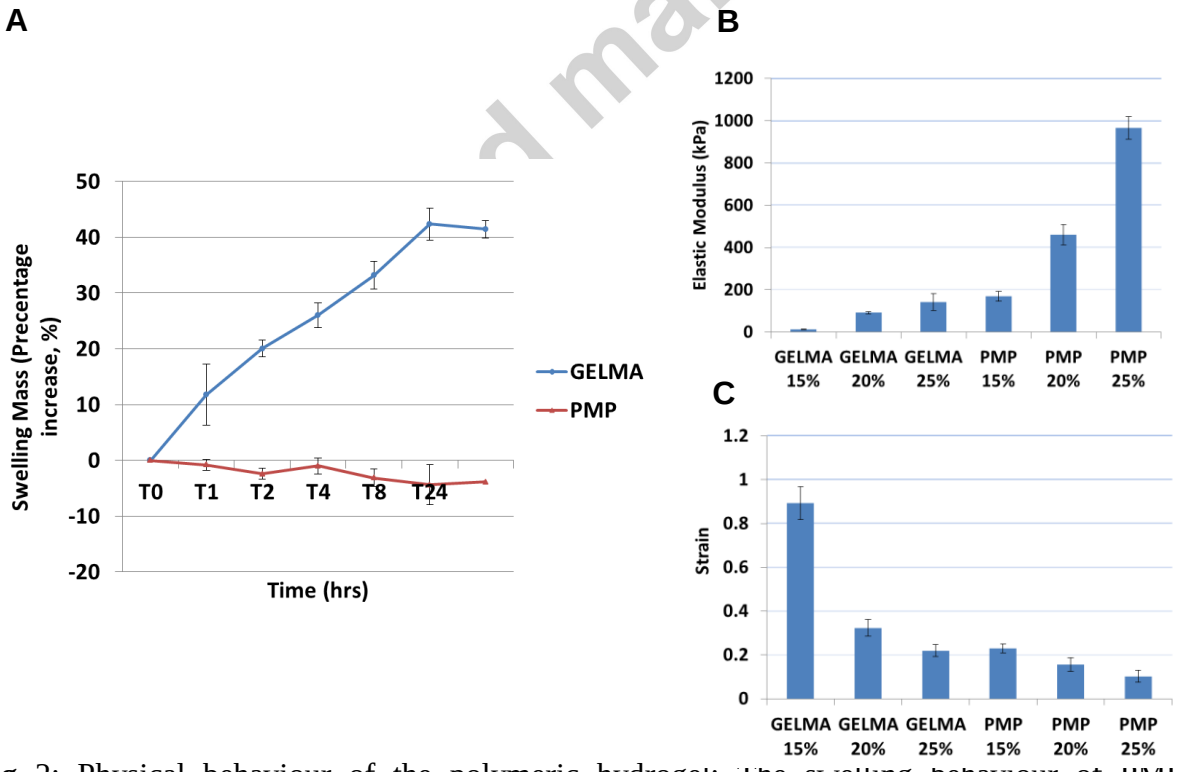

Fig 2: Physical behaviour of the polymeric hydrogel: The swelling behaviour of PMP hydrogel shows clearly that it does not undergo swelling even after 24 hours of incubation (A).

Mechanical properties were measured using texture analyser were the elastic moduli, and strain were calculated from force and distance (B and C).

The potential application of synthetic polymers, such as PMP, as cellular support materials for tissue regeneration in chronic wounds requires the polymer to not only support cell survival, but also proliferation and growth. When fibroblasts were seeded inside the PMP hydrogel cell viability remained over 90% for 7 days (Figure S1). However, the cells did not proliferate in the hydrogel over the same period, contrary to fibroblasts seeded in collagen or on 2D culture flasks (Figure 3). It is very probable that the chemical composition and inert nature of the polymer prevents cell attachment [30] which can be identified by the clear round morphology of the cells (Figure 3, B) unlike the stretched and elongated shape seen on cells seeded inside collagen (Figure 3, A).

The PMP polymer can be printed into a millimetre-precise shape with multiple layers with the aid of sacrificial thickening agent (gelatine). The printing, which utilises a 25 gauge needle (0.26 mm nominal inner diameter), did not influence cell viability or proliferation (Figure 3 E). The preferential cell proliferation points to the need for providing cell-spreading supporting environment to induce cell proliferation within the PMP hydrogel [31]. To do this, gelatine-methacrylate (gel-MA) coated PLGA microparticles (MPs) were mixed with the hydrogel solution before crosslinking.

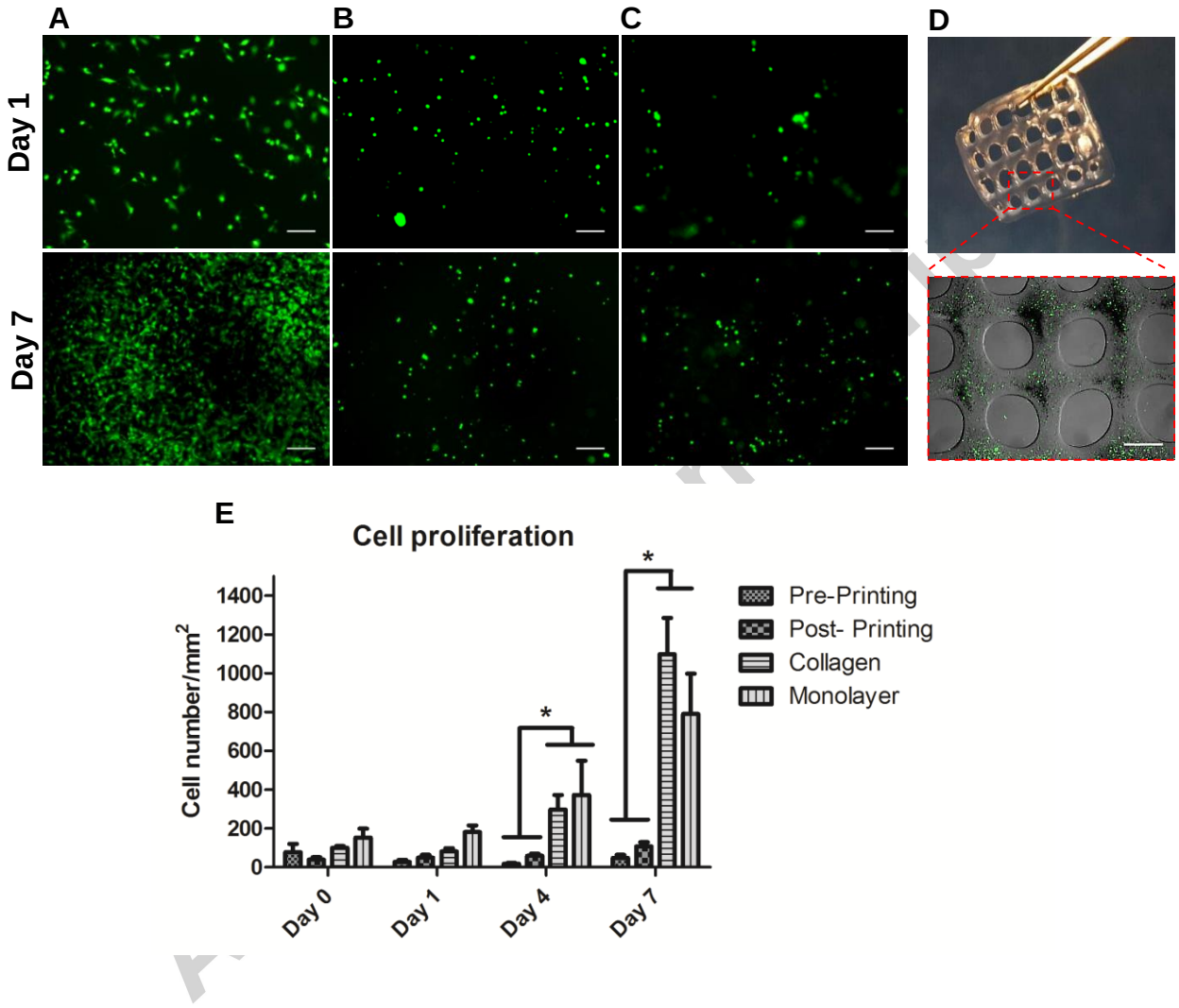

Fig 3: Cell proliferation rate of NIH/3T3 fibroblasts inside collagen (A), PMP (B) and PMP post-printing (C). Live to dead cell ratio were measured using live/dead assay and quantified with ImageJ. (Scale bar = 100 um). Image of printed PMP gel of multiple layers (top) and fluorescence microscope image (overlay) of a single layer (bottom) (Scale bar = 500 um) (D). Graph showing the proliferation rate of fibroblasts (monolayer: cells on tissue culture plate) over 7 days (E).

Poly (lactic-co-glycolic acid) microspheres were prepared by the commonly used emulsion based technique, as previously reported [32]. Low pressure oxygen plasma etching treatment was performed to introduce active oxygen species to the surface of the PLGA microspheres. Following plasma treatment, PLGA microspheres were dispersed in gel-MA (Gelatine-Methacrylate) solution to complete the surface modification. The gel-MA modification step was inducted to enhance cell adhesion and potentially, to enable further grafting of bioactive molecules. Following modification, two methods were used to determine gel-MA binding to the microspheres; Time of Flight Secondary Ion Mass Spectrometry (ToF-SIMS) and fluorescence microscopy (Figure 4). There was a clear distinction between unmodified and gel-MA coated MPs as seen in ion mapping images (Figure 4 A). Unmodified microspheres show complete coverage of red C_2H_5O surface while gel-MA modified microspheres show clear coating of Cyan CNO^- attributed to gel-MA. This is supported by fluorescence images that show near-complete coverage of FITC-labelled gel-MA on PLGA microspheres surfaces (Figure 4 B).

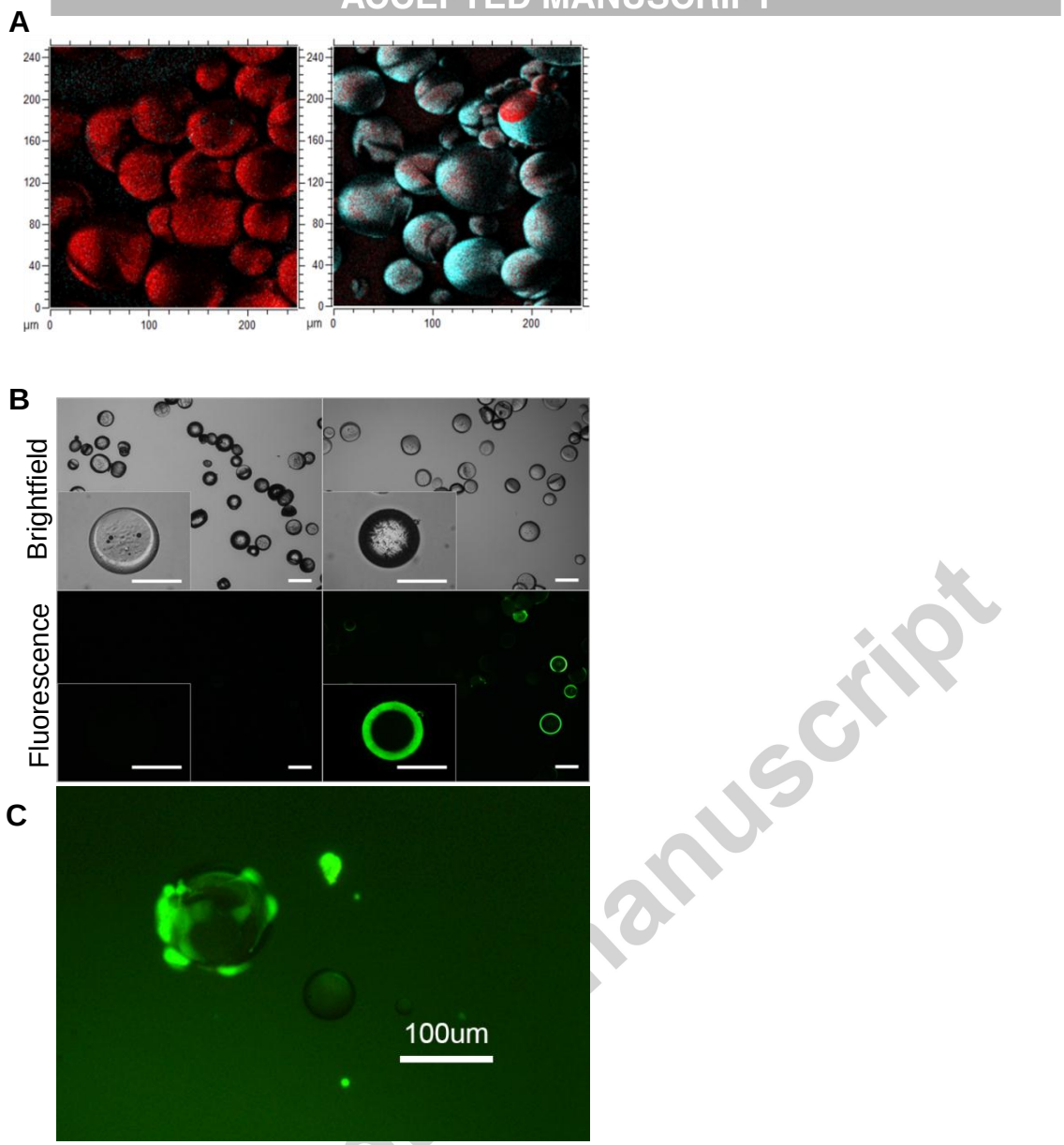

Fig 4: Characterisation of PLGA particles coated with gel-MA. (A) Ion mapping images of (C2H5O-) and (CNO-) ions related to PLGA (red, left) and gel-MA (cyan, right) respectively, show homogenous distribution of gel-MA ions on the surface of plasma modified microspheres. On the other hand, no clear sign of gel-MA specific ions can be seen on non-modified PLGA microspheres. (B) Fluorescent images of cross-sectioned microspheres show the depth of surface modification effect using Fit-C labelled gel-MA. Considerable amount of Fit-C gel-MA can be observed on the surface on the plasma treated microspheres). (Scale bar = 100 µm).

There was clear improvement in cell proliferation after the inclusion of 15% gel-MA coated PLGA MPs. Although there still remains significantly higher proliferation in collagen and

monolayer cultures, the cell number doubled in the presence of the MPs from 200 cells/mm^2 to 400 cells/mm^2 with MPs at day 7 (Figure 5). Moreover, 3D printing of the cell-laden PMP hydrogel with MPs did not induce observable apoptosis and thus, there was no significant difference between cell number before and after printing at day 7. The morphology of the cells has also changed to resemble more that seen in collagen as a result of cell adhesion to the gel-MA coated MPs. The results suggest that inclusion cell adhering surfaces such as the gel-Ma coated surface on MPs can increase cell proliferation in inert hydrogels such as PMP.

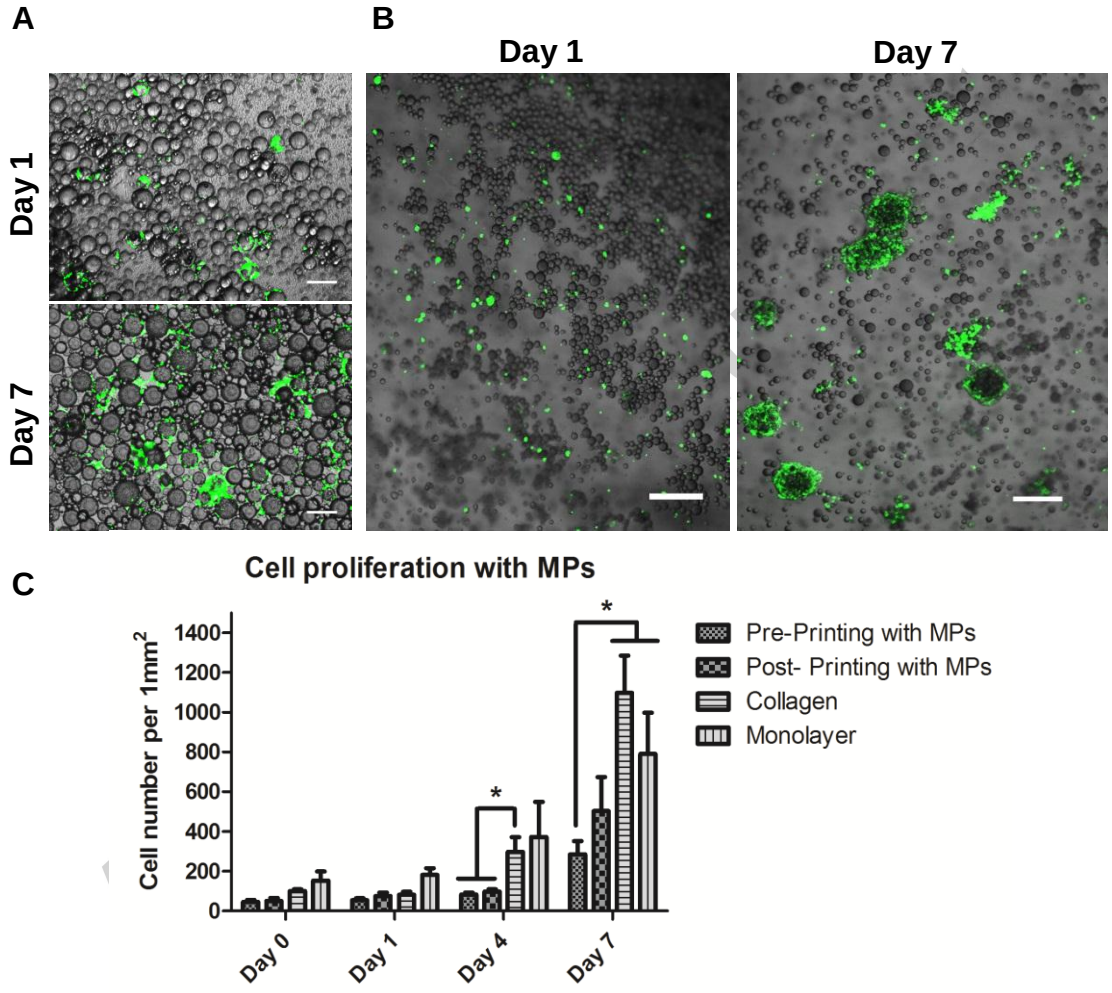

Fig 5: Proliferation rate of NIH/3T3 fibroblasts in PMP hydrogel loaded gel-MA coated MPs. Overlay of fluorescence and bright field images in 2D culture (Scale bar = 100 um) (A) and 3D culture (Scale bar = 200 um) (B) show the influence of gel-MA coated MPs on cell proliferation rate. Graphical representation of cell proliferation rate after printing (C) show no statistical significance between normal PMP gel with MPs or printed gel with MPs.

Conclusion

In summary, we have successfully synthesised a photocrosslinkable, 3D printable PEG based hydrogel using DE-ATRP that is nontoxic, nonimmunogenic and its inert nature circumnavigated by the impregnation of gelatine-methacrylate (gel-MA) coated PLGA microparticles to promote cell adhesion and proliferation. The inclusion of the MPs increased cell proliferation in the hydrogel which suggests that is method is a good alternative to chemical modification such as the use of RGD peptides which have selectivity and reliability issues. Moreover, the polymer can be 3D printed into precise shapes using layer-by-layer 3D printing without damaging the cells in the process. These results are preliminary and prove the potential of combinatorial use of synthetic hydrogels and microparticles in the 3D printing of tissues.

Acknowledgements
We would also like to thank the EU Marie Curie COFUND scheme for sponsoring Dr Ahmed Aied's fellowship.

References

1. Hutmacher, D.W., M. Sittinger, and M.V. Risbud, *Scaffold-based tissue engineering: rationale for computer-aided design and solid free-form fabrication systems.* Trends in Biotechnology, 2004. **22**(7): p. 354-362.
2. Hull, C.W., *Apparatus for production of three-dimensional objects by stereolithography*. 1986, Google Patents.
3. Boland, T., W.C. Wilson, and T. Xu, *Ink-jet printing of viable cells*. 2006, Google Patents.
4. Wilson, W.C., Jr. and T. Boland, *Cell and organ printing 1: protein and cell printers.* Anat Rec A Discov Mol Cell Evol Biol, 2003. **272**(2): p. 491-6.
5. Xu, T., et al., *Inkjet printing of viable mammalian cells.* Biomaterials, 2005. **26**(1): p. 93-99.
6. Zopf , D.A., et al., *Bioresorbable Airway Splint Created with a Three-Dimensional Printer.* New England Journal of Medicine, 2013. **368**(21): p. 2043-2045.
7. Hutmacher, D.W., M. Sittinger, and M.V. Risbud, *Scaffold-based tissue engineering: rationale for computer-aided design and solid free-form fabrication systems.* Trends in Biotechnology. **22**(7): p. 354-362.
8. Hutmacher, D.W., *Scaffold design and fabrication technologies for engineering tissues — state of the art and future perspectives.* Journal of Biomaterials Science, Polymer Edition, 2001. **12**(1): p. 107-124.

9. Khalil, S., J. Nam, and W. Sun, *Biopolymer deposition for freeform fabrication of tissue engineered scaffolds.* Proceedings of the Ieee 30th Annual Northeast Bioengineering Conference, 2004: p. 136-137.
10. Jakab, K., et al., *Three-dimensional tissue constructs built by bioprinting.* Biorheology, 2006. **43**(3-4): p. 509-513.
11. Peltola, S.M., et al., *A review of rapid prototyping techniques for tissue engineering purposes.* Annals of Medicine, 2008. **40**(4): p. 268-280.
12. Zhao, Y., et al., *The influence of printing parameters on cell survival rate and printability in microextrusion-based 3D cell printing technology.* Biofabrication, 2015. **7**(4).
13. Delaney, J.T., et al., *Reactive inkjet printing of calcium alginate hydrogel porogens-a new strategy to open-pore structured matrices with controlled geometry.* Soft Matter, 2010. **6**(5): p. 866-869.
14. Xu, T., et al., *Viability and electrophysiology of neural cell structures generated by the inkjet printing method.* Biomaterials, 2006. **27**(19): p. 3580-3588.
15. Bajaj, P., et al., *3D Biofabrication Strategies for Tissue Engineering and Regenerative Medicine.* Annual Review of Biomedical Engineering, Vol 16, 2014. **16**: p. 247-276.
16. Rose, J.B., et al., *Gelatin-Based Materials in Ocular Tissue Engineering.* Materials, 2014. **7**(4): p. 3106-3135.
17. Dong, Y.X., et al., *Dual stimuli responsive PEG based hyperbranched polymers.* Polymer Chemistry, 2010. **1**(6): p. 827-830.
18. Seiler, M., *Hyperbranched polymers: Phase behavior and new applications in the field of chemical engineering.* Fluid Phase Equilibria, 2006. **241**(1-2): p. 155-174.
19. Voit, B., *New developments in hyperbranched polymers.* Journal of Polymer Science Part a-Polymer Chemistry, 2000. **38**(14): p. 2505-2525.
20. Veronese, F.M., *Peptide and protein PEGylation: a review of problems and solutions.* Biomaterials, 2001. **22**(5): p. 405-417.
21. Kobayashi, H., et al., *Positive effects of polyethylene glycol conjugation to generation-4 polyamidoamine dendrimers as macromolecular MR contrast agents.* Magnetic Resonance in Medicine, 2001. **46**(4): p. 781-788.
22. Nichols, J.W., et al., *Cell-laden microengineered gelatin methacrylate hydrogels.* Biomaterials, 2010. **31**(21): p. 5536-44.
23. Tai, H., et al., *Thermoresponsive and photocrosslinkable PEGMEMA-PPGMA-EGDMA copolymers from a one-step ATRP synthesis.* Biomacromolecules, 2009. **10**(4): p. 822-8.
24. Lee, S., X. Tong, and F. Yang, *The effects of varying poly(ethylene glycol) hydrogel crosslinking density and the crosslinking mechanism on protein accumulation in three-dimensional hydrogels.* Acta Biomater, 2014. **10**(10): p. 4167-74.
25. Lee, S., X. Tong, and F. Yang, *Effects of the poly(ethylene glycol) hydrogel crosslinking mechanism on protein release.* Biomater Sci, 2016. **4**(3): p. 405-11.
26. Weber, L.M., C.G. Lopez, and K.S. Anseth, *Effects of PEG hydrogel crosslinking density on protein diffusion and encapsulated islet survival and function.* J Biomed Mater Res A, 2009. **90**(3): p. 720-9.
27. Bohari, S.P., D.W. Hukins, and L.M. Grover, *Effect of calcium alginate concentration on viability and proliferation of encapsulated fibroblasts.* Biomed Mater Eng, 2011. **21**(3): p. 159-70.
28. Mazzoccoli, J.P., et al., *Mechanical and cell viability properties of crosslinked low- and high-molecular weight poly(ethylene glycol) diacrylate blends.* J Biomed Mater Res A, 2010. **93**(2): p. 558-66.

29. Basta, G., et al., *Long-term metabolic and immunological follow-up of nonimmunosuppressed patients with type 1 diabetes treated with microencapsulated islet allografts: four cases.* Diabetes Care, 2011. **34**(11): p. 2406-9.
30. Tan, F., et al., *Fabrication of positively charged poly(ethylene glycol)-diacrylate hydrogel as a bone tissue engineering scaffold.* Biomed Mater, 2012. **7**(5): p. 055009.
31. Garcia, A.J., M.D. Vega, and D. Boettiger, *Modulation of cell proliferation and differentiation through substrate-dependent changes in fibronectin conformation.* Molecular Biology of the Cell, 1999. **10**(3): p. 785-798.
32. White, L.J., et al., *Accelerating protein release from microparticles for regenerative medicine applications.* Mater Sci Eng C Mater Biol Appl, 2013. **33**(5): p. 2578-83.